Black hole tidal charge constrained by strong gravitational lensing

Zsolt Horváth[1,2†], **László Á. Gergely**[1,2‡]

[1] Department of Theoretical Physics, University of Szeged, Tisza L krt 84-86, Szeged 6720, Hungary

[2] Department of Experimental Physics, University of Szeged, Dóm tér 9, Szeged 6720, Hungary

[†]zshorvath@titan.physx.u-szeged.hu; [‡]gergely@physx.u-szeged.hu

Abstract. Spherically symmetric brane black holes have tidal charge, which modifies both weak and strong lensing characteristics. Even if lensing measurements are in agreement with a Schwarzschild lens, the margin of error of the detecting instrument allows for a certain tidal charge. In this note we derive the respective constraint on the tidal charge of the supermassive black hole (SMBH) in the center of our galaxy, from the radius of the first relativistic Einstein ring, emerging in strong lensing. We find that even if general relativistic predictions are confirmed by high precision strong lensing measurements, SMBHs could have a much larger tidal charge, than the Sun or neutron stars.

1. Introduction

The Galactic Center is a highly dynamical region of the galaxy, however hard to resolve due to source confusion. Absorbing gas and dust is hiding the Galactic Center from Earth observers. Consequently, most of the knowledge about this part of our galaxy comes from observations in radio and infrared. A comprehensive introduction on the Galactic Center can be found in Ref. [1]. It has been estimated [2] that cold dark matter remnants of 1000 solar masses ($M_\odot$) and compact star remnants of 1000 $M_\odot$ reside in the inner 0.01 parsec (pc‡) region of the Galactic Center. The star population in the inner 0.04 pc, the SgrA* stellar cluster consists of B stars [3]. These are the remains from the dynamical process ejecting the hypervelocity stars of the Galactic halo [4]. In the distance range $0.04-0.5$ pc Wolf Rayet and OB giant stars are found, all aged about 6 million years [5].

The Galactic Center is dominated by a Supermassive Black Hole (SMBH), with mass $\mathcal{M}_{BH}$=4.31 $\times$ 10^6 $M_\odot$ and distance from the Sun r_{BH} = 8330 pc, respectively [6]. The orbits of nearby stars depend on the mass and spin of the SMBH. These characteristics can be deduced from rigurous observations of stellar orbits [7],[8].

The first measurements of proper motions of stars within 2400 AU from the center of our Galaxy was published in Ref. [9]. A detailed review of the results of 16 years of monitoring stellar orbits around the SMBH using NIR techniques can be found in Ref. [10]. An animation of the orbits of individual stars around the SMBH has been produced from the images recorded between 1995 and 2011 by the UCLA Galactic Center Group [11].

Very recently a study of the stellar orbits around the Galactic Center by the NACO 9, SINFONI 10 and 11 observation programmes, performed with the Very Large Telescope (VLT), proved the existence of a gas cloud approaching the center of Sgr A* [6]. This can be seen from the redshifted H and He emission lines in the spectrum of the L' infrared band. The temperature of the gas cloud is 550 K, its luminosity 5 $L_\odot$ [6] and its mass of order 10^{24} kg [12]. Table 1. of Ref. [6] summarizes the orbital elements of the cloud, implying an orbital period of 137 $\pm$ 11 years. The velocity of the cloud increased from 1200 km/s in 2004 to 2350 km/s in 2011. The gas cloud began to disrupt in 2009 due to tidal shearing arising from the SMBH's gravitational force. Its shorter characteristic size is either marginally resolved or unresolved, smaller than 24 milliarcsecond (mas). Its longer size is 46 $\pm$ 1 mas derived from the angular distance between the redshifted and blueshifted margins of the cloud. This is consistent with the photometrical width at half-maximum 42 ± 1 mas (2008) and 38 ± 1.6 mas (2011) of the cloud. It will reach the pericenter in 2013, at about 3140 times the event horizon of the SMBH. Only the two stars S2 and S14 have come closer to the black hole since the monitoring started in 1992 [6].

Light collected by all four telescopes of the VLT was successfully combined for the first time in 2011, using a new generation instrument in the VLT Interferometer,

‡ 1 pc = 206260 astronomical units (AU)

PIONIER [13]. The design of another instrument, GRAVITY has reached completion as well [14]. This will be able to use the four telescopes as an interferometer in the near-infrared (NIR) band. The astrometrical accuracy strongly depends on the number of sources in the field of view, the source confusion being the main factor of the uncertainty of position measurement [15]. The statistical properties of the stars at the centre of the Galaxy make it plausible that at least three stars could be observable at any time in GRAVITY's field of view [14]. GRAVITY will perform astrometry with 12 microarcsecond (μas) precision in the K band up to 15 magnitudes [14]. The margin of error of its measurements will be therefore

$$\Delta\Theta = 12 \times 10^{-6} \text{ as} . \tag{1}$$

From the numerous scientific applications of GRAVITY, described in Section 3 of Ref. [14], the observation of relativistic motions near the horizon of Sgr A* will be of uttermost importance.

By such observations of NIR flares even the metric near the horizon can be determined [16]. A submm-VLBI array should be able to actually resolve Sgr A* showing its event horizon as a shadow [17]. According to Ref. [7] the no-hair theorem can be tested.

The planned accuracy of future radio instruments is compatible or even better (of order μas for the Square Kilometre Array [18] however for lensing phenomena we are primarely interested in NIR measurements. (Lensing observations in NIR are common, for an examle see Ref. [19].)

With increasing measurement accuracy and the possibility of direct observations of the horizon of the SMBH at the Galactic Center the possibility of testing general relativistic predictions emerges. Even if a certain measurement confirms them, the measurement accuracy of a specific instrument will allow for certain margin of error for any additional parameter. From among the various possibilities we will test here the existence of a tidal charge, an imprint of the possible 5-dimensional nature of gravity in a brane-world scenario [20], [21]. A tidal charge emerges from the Weyl curvature of a 5-dimensional space-time in which our 4-dimensional observable world is embedded. Such a tidal charged black hole solution on a brane was found in Ref. [22]. The electric part of the Weyl curvature, non-standard model 5-dimensional fields, asymmetric embedding and a varying brane tension all could act as sources of the effective Einstein equation [23], [24], [25]. In consequence unusual cosmologies may emerge [26], [27]. Remarkably, the Weyl curvature source term could replace dark matter [28], [29].

Light deflection and weak gravitational lensing by tidal charged brane black holes was investigated in Refs. [30], [31], [32]. One of the results of these investigations was a strict limit imposed on the tidal charge from Solar System measurements.

In this paper we study strongly relativistic orbits in the Galactic Center. We focus on 1-loop photon trajectories, as depicted on Fig. 1. We summarize the basic equations concerning the one-loop null geodesics in spherically symmetric, static space-times in Section 2. The formation of the first relativistic Einstein ring, emerging due to strong

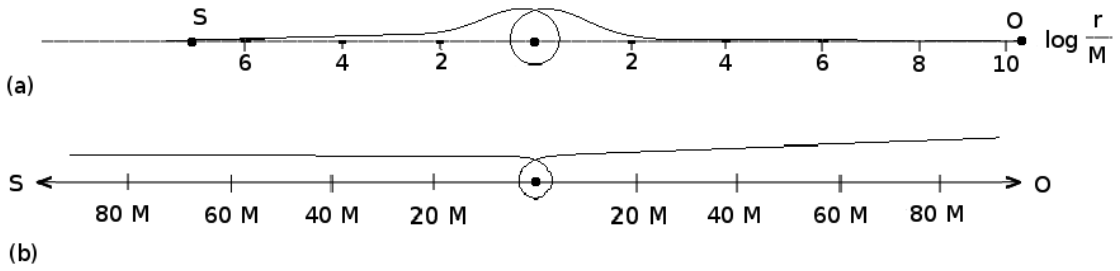

Figure 1. The trajectory of light along which the photons travel from the source S to the observer O, while turning around the lens L once, for $q = 0$, $D_L = 8600$ pc, $D_{LS} = 10$ pc. On panel (a) the whole geodesics is seen on logarithmic scale. The distorted region in the left and right side of the loop is magnified and shown on a linear scale on panel (b).

lensing by the SMBH in the center of our galaxy is discussed in Section 3, under the assumption, that the metric is the tidal charged brane black hole [22]. Then we discuss the possibility that the radius of this Einstein ring varies in the margin of error of GRAVITY in the infrared astrometry regime and allow for a non-vanishing tidal charge in this range.

We present our conclusions, which include the constraints on the tidal charge derived by this method, in Section 4.

2. Null geodesics and relativistic Einstein angles in spherically symmetric, static space-times

The general spherically symmetric, static metric is

$$ds^2 = g_{tt}dt^2 + g_{rr}dr^2 + r^2d\theta^2 + r^2sin^2\theta\ d\varphi^2\ . \tag{2}$$

Without reducing generality, we can restrict geodesic motions to the plane $\theta = \pi/2$. The (second order) radial geodesic equation can be replaced by the (first order) null condition

$$0 = g_{tt}\left(\frac{dt}{dp}\right)^2 + g_{rr}\left(\frac{dr}{dp}\right)^2 + g_{\varphi\varphi}\left(\frac{d\varphi}{dp}\right)^2\ , \tag{3}$$

where p is a parameter of the null curve. As the spherically symmetric, static metric does not depend on either of the coordinates t or φ, two constants of motion emerge by integration from the geodesic equations:

$$L = g_{\varphi\varphi}\frac{d\varphi}{dp}\ , \tag{4}$$

$$E = g_{tt}\frac{dt}{dp}\ . \tag{5}$$

L is the specific angular momentum of the photon [33], its dimension being [length^2], while Ec^4/G is the energy of the photon, the dimension of E being [length].

Then the rr term in Eq. (3) can be written in the form $g_{rr}\left(dr/d\varphi\right)^2 L^2/g_{\varphi\varphi}^2$, while the tt and $\varphi\varphi$ terms as E^2/g_{tt} and $L^2/g_{\varphi\varphi}$, respectively. Hence the radial equation becomes

$$0 = \frac{E^2}{g_{tt}} + g_{rr}\left(\frac{dr}{d\varphi}\right)^2 \frac{L^2}{g_{\varphi\varphi}^2} + \frac{L^2}{g_{\varphi\varphi}} \ . \tag{6}$$

By reordering the terms, we obtain the equation characterising the trajectory $r\left(\varphi\right)$:

$$\frac{dr}{d\varphi} = \pm\left[\frac{g_{\varphi\varphi}}{g_{rr}}\left(\frac{E^2}{L^2}\frac{g_{\varphi\varphi}}{-g_{tt}} - 1\right)\right]^{1/2} \ . \tag{7}$$

The sign differentiates between the incoming and outgoing parts of the path.§ The trajectory can be also expressed in terms of the dimensionless radial coordinate $R = r/M$.

We will seek a null geodesic curve along which the photons travel from the source S to the observer O, while turning around the lens L once (1-loop orbit). The source, the lens and the observer are on the same coordinate line $\varphi = 0$, called the optical axis, more specifically L is the origin, S lies at $(\varphi = 0, r = D_{LS})$, while O at $(\varphi = \pi, r = D_L)$. Then the trajectory $r\left(\varphi\right)$ of the photon is a decreasing function from $r = D_{LS}$ to some distance $r = r_{min}$, then increases to $r = D_L$. This distance of minimal approach $r_{min} = r\left(\varphi_{min}\right)$ is a solution of the equation [31]

$$\frac{dr}{d\varphi}\left(\varphi_{min}\right) = 0 \ . \tag{8}$$

For such a one-loop path the total change of the polar angle φ from S to O is $\pi + 2\pi$. The function $\varphi\left(p\right)$ is invertible either in the range $\pi \leq \varphi \leq 2\pi$ (as there is only one r for each such φ), or in both monotonous parts of the path $r\left(\varphi\right)$. (In these monotonic regions for any φ there is again only one corresponding r for each φ.)

In what follows, we derive the angular radius Θ_E of the first relativistic Einstein ring (the image created by all these 1-loop orbits). This is defined as the angle between the optical axis SO and the tangent of the geodesic curve at the point O. Since at the point O the radial vector $\partial/\partial R$ is parallel with the optical axis, we define the observable Einstein angle Θ_E as the angle between the vector $\partial/\partial R$ and the tangent of the curve $R\left(\varphi\right)$ at the point O.

In the following derivation every vector field is evaluated at O. The scalar product (given by the metric (2)) of the base vector $\partial/\partial R$ and the tangent $\partial/\partial p$ can be computed in two independent ways. First, from the general definition of the (Euclidian) scalar product of two vectors:

$$\begin{aligned}\frac{\partial}{\partial R}\cdot\frac{\partial}{\partial p} &= \left|\frac{\partial}{\partial R}\right|\left|\frac{\partial}{\partial p}\right|\cos\Theta_E \\ &= \sqrt{g_{RR}\left(D_L\right)}\sqrt{\left(\frac{\partial R}{\partial p}\right)^2 g_{RR}\left(D_L\right) + \left(\frac{\partial\varphi}{\partial p}\right)^2 g_{\varphi\varphi}\left(D_L\right)}\cos\Theta_E \ .\end{aligned} \tag{9}$$

§ Eq. (8.5.6) of Ref. [34] presents this equation in a reciprocal and integrated form, with the source and the observer placed at infinity, featuring r_{min} instead of the impact parameter L/E; and employing the specific choice $g_{\varphi\varphi} = r^2$.

Second, from the decomposition of the tangent vector in the polar coordinate system we get:

$$\frac{\partial}{\partial R}\cdot\frac{\partial}{\partial p}=\frac{\partial}{\partial R}\cdot\left(\frac{\partial R}{\partial p}\frac{\partial}{\partial R}+\frac{\partial\varphi}{\partial p}\frac{\partial}{\partial\varphi}\right)=\frac{\partial R}{\partial p}\frac{\partial}{\partial R}\cdot\frac{\partial}{\partial R}=\frac{\partial R}{\partial p}g_{RR}\left(D_L\right)\ . \quad (10)$$

Putting the right hand sides equal, we obtain

$$\Theta_E: \quad =arccos\frac{\frac{\partial R}{\partial p}\sqrt{g_{RR}\left(D_L\right)}}{\sqrt{\left(\frac{\partial R}{\partial p}\right)^2 g_{RR}\left(D_L\right)+\left(\frac{\partial\varphi}{\partial p}\right)^2 g_{\varphi\varphi}\left(D_L\right)}}$$

$$=arccos\left[\frac{\left(\frac{dR}{d\varphi}\right)^2 g_{RR}}{\left(\frac{dR}{d\varphi}\right)^2 g_{RR}+g_{\varphi\varphi}}\right]^{1/2}\ . \quad (11)$$

In the last step the parametrization of the curve $R\left(\varphi\right)$ was eliminated by multiplying both the numerator and the denominator by $dp/d\varphi$ (the angle between a vector and a curve must be independent from the parametrization). The right hand side of Eq. (11) is evaluated at $R=D_L/M$ (the location of the observer).

3. The first relativistic Einstein ring and constraints on the tidal charge

The tidal charged black hole [22] generalizes the Schwarzschild solution by allowing for a tidal charge parameter q in the metric function

$$g_{tt}=-\frac{1}{g_{rr}}=-1+\frac{2M}{r}-\frac{q}{r^2} \quad (12)$$

of the spherically symmetric, static space-time (2). This emerges as a vacuum solution of the effective Einstein equation on a brane with q allowed to take either sign. For $q<0$ there is a horizon at $M+(M^2-q)^{1/2}$, while for $0<q<M^2$ there are two horizons, at $M\pm(M^2-q)^{1/2}$. When $q=M^2$ the two horizons coincide at M , while for $q>M^2$ the metric describes a naked singularity.

The trajectory of a photon, Eq. (7) in this space-time becomes

$$\frac{dR}{d\varphi}=\pm\left[\left(\frac{EM}{L}\right)^2 R^4-R^2+2R-\frac{q}{M^2}\right]^{1/2}\ , \quad (13)$$

Here the impact parameter L/E, normalized to M is dimensionless, similarly as R. The minimal dimensionless distance $R_{min}:=r_{min}/M$ (larger than the outer horizon of the lens) is a root of the polynomial emerging from Eq. (13) by setting to zero the left hand side.

The Einstein angle (11) then becomes

$$\Theta_E=arccos\left\{1-\left(\frac{L}{ME}\right)^2\left[\left(\frac{M}{D_L}\right)^2-2\left(\frac{M}{D_L}\right)^3+\frac{q}{M^2}\left(\frac{M}{D_L}\right)^4\right]\right\}\ . \quad (14)$$

Next we assume a stellar source on the optical axis defined by the SMBH and the GALAXY detector, at a distance D_{LS} varying in the range [10 pc, 100000 pc] and a

Table 1. Column 1.: the tidal charge, column 2.: the angular radius of the first relativistic Einstein ring, column 3.: the normalized radius of the horizon, column 4: the minimal distance $R_{min} = r_{min}/M$, larger than the horizon in each case, column 5.: the parameter L/ME, column 6.: the normalized tidal charge.

$q\,[10^{20}\ m^2]$	$\Theta_E\ [\mu as]$	r_H/M	r_{min}/M	L/ME	q/M^2
-1.815141	38	3.345	4.924	7.706	-4.5
-1.613458	37	3.236	4.772	7.496	-4.0
-1.411776	36	3.121	4.612	7.275	-3.5
-1.210094	35	3.000	4.443	7.043	-3.0
-1.008411	34	2.870	4.265	6.797	-2.5
-0.806729	32	2.732	4.073	6.535	-2.0
-0.605047	31	2.581	3.866	6.252	-1.5
-0.403364	29	2.414	3.639	5.943	-1.0
-0.201682	28	2.224	3.385	5.598	-0.5
0.000000	26	2.000	3.090	5.202	0.0
0.524374	14	n. s.	1.446	3.207	1.3

photon trajectory with one loop about the SMBH. Each value of L/ME determines a null geodesic curve by Eq. (13), however for most of the values the resulting curve does not reproduce the desired lensing geometry (e.g. the boundary conditions set by S and O). Therefore one has to 'fine-tune' L/ME to generate the specific curve which satisfies the conditions preset by the 1-loop orbit. We have done this in the following way. After setting the tidal charge q and the distance D_{LS}, we choose some value for the L/ME (it turned out to be useful to chose it between 1 and 10). Then we evolve the differential equation (13) numerically with this value and calculate the change in the polar angle φ which emerges, while the photon travels from the distance D_{LS}/M to R_{min} then further to D_L/M. For the choice $L/ME = 10$ this angular change was too large ($\Delta\varphi > 3\pi$) for any $q \in [-5\ M^2,\ +1.3\ M^2]$ and $D_{LS} \in$[10 pc, 100000 pc]. Therefore we have to reduce the value of L/ME, and repeat the procedure, until it yields $\Delta\varphi = 3\pi$ (with 10^{-12} rad accuracy). In this iterative way we obtain the dimensionless impact parameter for the considered 1-loop photon orbit. Finally we insert the correct value of L/ME in Eq. (14) and calculate the size of the first relativistic Einstein ring.

The values of both L/ME and Θ_E found for $D_{LS} = 10$ pc and $q \in [-5\ M^2,\ +1.3\ M^2]$ are listed in Table 1. The colums are (1): the discrete values of the tidal charge in the range studied, (2): the angular radius of the first relativistic Einstein ring, (3): the horizon radius normalized by mass (when applicable), or naked singularity (n. s.) for $M^2 < q$, (4): the normalized minimal distance from the lens $R_{min} = r_{min}/M$, (5): the dimensionless impact parameter L/ME, (6): the tidal charge normalized by M^2. The $q = 0$ line in the table reproduces the Enstein angle calculated for a Schwarzschild lens in Ref. [35], $\Theta_E(0, D_{LS}) = 26\ \mu$as.

We have checked that by varying D_{LS} the values of the Einstein angles change by less than 1μas (this is how the agreement with the result of Ref. [35], calculated for $D_{LS} = 8600$ pc, is acheved). Also note that the values of the tidal charge were varied such as the Einstein radius changes at most with the value (1), the designed margin of error of the measurements of the detecting instrument, GRAVITY, as compared to the Schwarzschild value. This allows for the limits $q_{\rm min}$ and $q_{\rm max}$ given by

$$\Theta_E(q_{min}, D_{LS}) = \Theta_E(0, D_{LS}) + \Delta\Theta \ ,$$
$$\Theta_E(q_{max}, D_{LS}) = \Theta_E(0, D_{LS}) - \Delta\Theta \ . \qquad (15)$$

Thus a tidal charge falling in the range $q \in [-1.815,\ 0.524] \times 10^{20}$ m^2 will be consistent with measurements of the first relativistic Einstein ring generated by sources opposite to us with respect to the central SMBH.

4. Concluding Remarks

Bounds on the tidal charge of various astrophysical objects were derived earlier in the literature. For neutron stars a limit of $|q| < 10^7$ m^2 was establised in Ref. [36] from orbital models of high-frequency quasiperiodic oscillations observed in neutron star binary systems. From the constraint on the brane tension presented by Eq. (30) in Ref. [37] a weaker limit for *negative* tidal charges emerges in the following way. The junction condition (Eq. (35) in Ref. [37]) of the uniform density star and its exterior represented by the tidal charged metric associates a tidal charge to the limiting brane tension, provided the junction radius is known.. The latter is bounded from below by the compactness limit (the inequality (31) in Ref. [37]). This gives $0 > q > -9.730 \times 10^8$ m^2. The strongest constraint for the Sun was found in Ref. [30] from the perihelion precession of the Earth, $|q| \leq 6 \times 10^3$ m^2. Light deflection measurements impose a milder restriction on the tidal charge of the Sun, $|q| \leq 2.966 \times 10^9$ m^2 [31].

The question comes, whether experiments available in the near future targeting the observation of much larger objects in the Universe, where strong gravitational lensing could be relevant, would lead to other limits. Such tests concerning relativistic Einstein rings will be achievable by measurements of the high-precision designed instrument GRAVITY. We have studied the formation of the first relativistic Einstein ring in the tidal charged black hole geometry on the brane. For this we have specified the lensing geometry for the SMBH in the center of our galaxy, considered as a lens and for a light source opposite to us with respect to this SMBH, as a source. Following a similar logic to Refs [30], [31], thus assuming that strong lensing experiments will confirm the general relativistic predictions, but measurements error will still allow for some tidal charge, we have found a much larger value for the possible tidal charge of the SMBH in the Center of the Galaxy. Despite the instrument possibly confirming the Schwarzschild geometry within measurement accuracy, the range $q \in [-1.815,\ 0.524] \times 10^{20}$ m^2 of the tidal charge is still allowed, as the modifications induced by such a tidal charge fall within the designed instrument GRAVITY's margin of measurement error

Table 2. Bounds on the tidal charge normalized by mass square from observations in the Solar System (first column) [30], constraints from orbital models of high-frequency quasiperiodic oscillations observed in neutron star binary systems [36] (second column), constraints on brane tension and the compactness limit of neutron stars (third column) [37], and finally, forthcoming strong lensing observations on the Galactic SMBH (fourth column), derived in this paper. Clearly, Solar System constraints are the strongest, neutron star bounds the weakest, while the neutron star binary and SMBH lensing constraints are of the same order of magnitude.

object	Solar System	neuton star binary	neuton star	SMBH
$\lvert q/M^2\rvert_{max}$	0.003	2.339	227.647	4.485

We have additionally checked that the second and third relativistic rings (with $\Delta\varphi = 5\pi, 7\pi$, respectively) lead to similar results on the allowed range of q, as the first ring. We explain this by the relativitic rings being situated quite close to each other (within 0.03 μas).

Although the derived constraint on q is much weaker than those from neutron stars or Solar System observations, the dimensionless quantity q/m^2 is not very much different 2. In fact for this quantity the neutron stars constraints are the weakest, and the Solar System constraints the strongest, while both the neutron star binary systems and the SMBH strong lensing considerations presented in this paper gave comparable constraints.

We conclude with the remark that even if general relativistic predictions on the Galactic SMBH are confirmed by high precision measurements, our investigations show that SMBHs could have a much larger tidal charge, than the Sun or neutron stars.

Acknowledgements

ZsH was supported by the European Union and co-funded by the European Social Fund through Grant No. TMOP 4.2.2/B-10/1-2010-0012. LG was partially supported by COST Action MP0905 "Black Holes in a Violent Universe".

5. References

[1] www.astro.ucla.edu/˜ghezgroup/gc/journey/index.shtml (2006).

[2] M. Morris, *ApJ* **408**, 496 (1993); J. Miralda-Escude, A. Gould, *ApJ* **545**, 847 (2000); P. Gondolo, J. Silk, *Phys. Rev. Lett.* **83**, 1719 (1999); P Ullio et al., *Phys. Rev. D* **64**, 43504 (2001); D. Merritt et al., *PRL* **88**, 191301 (2002); O. Y. Gnedin, J. R. Primack, *PRL* **93**, 061302 (2004); G. Bertone, D. Merritt, *PRD* **72**, 103502 (2005).

[3] A. Ghez et al., *ApJ* **586**, L127 (2003); F. Eisenhauer et al., *ApJ* **628**, 246-259 (2005); T. Do et al., *ApJ* **691**, 1021 (2009).

[4] W. Brown et al., *ApJ* **622**, L33 (2005); *ApJ* **671,** 1708 (2007); *ApJ* **690**, L69 (2009); H. Hirsch et al., *A&A* **444**, L61 (2005); H. Edelmann et al, *ApJ* **634**, L181 (2005).

[5] A Krabbe et al., *ApJ* **447**, L95 (1995); R. Blum et al., *ApJ* **441**, 603 (1995); P. Tamblyn et al.,

ApJ **456**, 206 (1996); F. Najarro et al., *A&A* **325**, 700 (1997); T. Paumard et al., *ApJ* **643**, 1011 (2006).
[6] S. Gillessen et al., *Nature* **481**, 51–54 (2012).
[7] C. M. Will, *ApJL* **674**, L25 (2008).
[8] D. Merritt, T. Alexander, S. Mikkola, C. M. Will, *Phys. Rev.* **D 81**, 062002 (2010)..
[9] A. Eckart, R. Genzel, *MNRAS* **284**, 576 (1997).
[10] S. Gilessen et al., *ApJ* **692**, 1075 (2009).
[11] www.astro.ucla.edu/~ghezgroup/gc/pictures/orbitsMovie.shtml (2011).
[12] Y. D. Xu, R. Narayan, E. Quataert, F. Yuan, F. K. Baganoff, *ApJ* **640**, 319–326 (2006).
[13] www.eso.org/public/announcements/ann11021 (2011).
[14] S. Gilessen et al., *Proceedings of the SPIE Astronomical Telescopes and Instrumentation Conference 2010* (2010), arXiv:1007.1612 [astro-ph.IM].
[15] A. Ghez et al., *The Galactic Center: A Laboratory for Fundamental Astrophysics and Galactic Nuclei,* ASTRO2010 White Paper, arXiv:0903.0383v1 [astro-ph.GA] (2009).
[16] D. Psaltis, *Measurements of Black Hole Spins and Tests of Strong-Field General Relativity*, *AIP Conf. Proc.* **714**, 29 (2004).
[17] H. Falcke, F. Melia, E. Agol, *ApJL* **528**, L13 (2000).
[18] T. Joseph, W. Lazio, J. M. Cordes, A. G. de Bruyn, J.-P. Macquart, *New Astron. Rev.* **48,** 1439-1457 (2004).
[19] F. Iwamuro et al., *Pub. Ast. Soc. Japan* **52**, 25 (2000).
[20] R. Maartens, K. Koyama, *Living Rev. Rel.* **13**, 5 (2010).
[21] R. Maartens, *Phys. Rev.* D **62**, 084023 (2000).
[22] N. Dadhich, R. Maartens, P. Papadopoulos, V. Rezania, *Phys. Lett B* **487**, 1 (2000).
[23] T. Shiromizu, K. Maeda, M. Sasaki, *Phys. Rev. D* **62,** 024012 (2000).
[24] L. Á. Gergely, *Phys. Rev. D* **68**, 124011 (2003).
[25] L. Á. Gergely, *Phys. Rev. D* **78,** 084006 (2008).
[26] L. Á. Gergely, R. Maartens, *Class. Quantum Grav.* **19**, 213 (2002).
[27] L. Á. Gergely, *Phys. Rev.* D **74**, 024002 (2006).
[28] T. Harko, K. S. Cheng, *Phys. Rev. D* **76**, 044013 (2007).
[29] M. K. Mak, T. Harko, *Phys. Rev. D* **70**, 024010 (2004); T. Harko, K. S. Cheng, *Astrophys. J.* **636**, 8 (2006); C. G. Boehmer, T. Harko, *Class. Quantum Grav.* **24**, 3191 (2007); L. Á. Gergely, T. Harko, M. Dwornik, G. Kupi, Z. Keresztes, *Mon. Not. Royal Astron. Soc.* **415**, 3275 (2011).
[30] G. C. Böhmer, T. Harko, F. S. N. Lobo, *Class. Quantum Grav.* **25**, 045015 (2008).
[31] L. Á. Gergely, Z. Keresztes, M. Dwornik, *Class. Quantum Grav.* **26**, 145002 (2009).
[32] Z Horváth, L Á Gergely, D Hobill, Class. *Class. Quantum Grav.* **27**, 235006 (2010).
[33] M. P. Hobson, G. P. Efstathiou, A. N. Lasenby, *General Relativity: An Introduction for Physicists* (Cambridge Univ. Press, 2006).
[34] S. Weinberg, *Gravitation and Cosmology: Principles and Applications of the General Theory of Relativity* (Wiley, New York, 1972).
[35] A. Bin-Nun, *Phys. Rev. D* **81**, 123011 (2010).
[36] A. Kotrlova, Z. Stuchlik, F. Török, *Class. Quant. Grav.* **25**, 225016 (2008).
[37] C. Germani, R. Maartens, *Phys. Rev. D* **64**, 124010 (2001).